Special Collection

Relating Bond Strength and Nature to the Thermodynamic Stability of Hypervalent Togni-Type Iodine Compounds

Vytor Pinheiro Oliveira,*[a] Bruna Luana Marcial,[b] Francisco B. C. Machado,[a] and Elfi Kraka[c]

The bond strength and nature of a set of 32 Togni-like reagents have been investigated at the M062X/def2-TZVP(D) level of theory in acetonitrile described with the SMD continuum solvent model, to rationalize the main factors responsible for their thermodynamic stability in different conformations, and trifluoromethylation capabilities. For the assessment of bond strength, we utilized local stretching force constants and associated bond strength orders, complemented with local features of the electron density to access the nature of the bonds. Bond dissociation energies varied from 31.6 to 79.9 kcal/mol depending on the polarizing power of the ligand trans to CF_3. Based on the analysis of the Laplacian of the density, we propose that the charge-shift bond character plays an important role in the stability of the molecules studied, especially for those containing I–O bonds. New insights on the trans influence and on possible ways to fine-tune the stability of these reagents are provided.

Introduction

Iodine is an exceptionally versatile element.[1] Monovalent iodine can be easily polarized by a transition metal[2] or an organic group,[3] leading to an anisotropic charge distribution. Collinear with the σ-bond, but at the opposite end, electron density is depleted, leaving a region of positive electrostatic potential called σ-hole[4] that can interact attractively with the negatively charged region of another molecule forming a non-covalent interaction called halogen bonding (XB). In the following, XB is also used for the term halogen bond. XB can also be described as a donor-acceptor interaction in which charge is transferred from the lone pair of a heteroatom or d_z orbital of a metal in a Lewis base into the empty σ* orbital of the halogenated moiety acting as a Lewis acid.[5] The latter definition has the advantage of providing a simpler explanation for XBs formed between I_2 and the metal center of a positively charged metallic pincer complex.[6] Although all halogens are able to form XBs, the higher polarizability of iodine leads, in general, to stronger XBs.[7] Iodine-based XB materials have been successfully applied for the development of liquid crystal, self-healing gels, luminescent functional materials,[8] supramolecular compartments for drug delivery, and sensors[3,9] to name a few materials. The usefulness of monovalent iodine is due to the capability of XBs to drive self-assembly in a predictable way[3] and the easiness in which the XBs can have their strength tuned by modifying the moiety attached to the iodine[7] or the Lewis base.[2a,6] For implementing a successful tuning strategy, a deeper understanding of the electronic structure based on reliable models[1a,8,10] is required.

In higher valence states, iodine compounds are called hypervalent, a term coined by Musher[11] to designate elements of the p-block in valence states in which the valence electrons cannot be satisfactorily depicted by a single Lewis structure without violating the octet rule.[12] Hypervalent iodine compounds are widely used in organic synthesis[13] and transition metal chemistry[14] and are well-known for their low toxicity and cost. Similar to transition metals, iodine can adopt various oxidation states, which allow a facile extension/reduction of its coordination sphere via oxidation and reduction reactions, ligand displacement from one position to another is also commonly observed. These properties make hypervalent iodine interesting alternatives, especially for pharmaceutical and agrochemical industry applications, in which the presence of transition metals is undesirable.[1d,15]

Trivalent iodine compounds (λ^3-iodanes) have recently received great attention in organofluoride chemistry for their ability to serve in group transfer reactions of trifluoromethyl or other fluorine-rich groups with various substrates.[16] Among λ^3-iodanes, Togni I and II are well-known versatile hypervalent iodine reagents, being used for trifluoromethylation of S, P, O, N and C centered nucleophiles including thiols, alcohols, amines, esters, phosphates, arenes, acetylenes, enones, ketones, lactones, and other substrates.[16,17]

Togni reagents are generally defined as aryl λ^3-iodanes benziodoxoles with a cyclic linker connecting the aromatic ring to iodine at a trans position with regard to CF_3 ligand via a five-member ring (see conformation i in Figure 1), which helps to

[a] Dr. V. P. Oliveira, Prof. Dr. F. B. C. Machado
Instituto Tecnológico de Aeronáutica (ITA)
Departamento de Química
São José dos Campos, 12228-900 São Paulo (Brazil)
E-mail: vytor3@gmail.com
[b] Prof. Dr. B. L. Marcial
Instituto Federal Goiano (IF Goiano)
Núcleo de Química
Campus Morrinhos, Goiás (Brazil)
[c] Prof. Dr. E. Kraka
Computational and Theoretical Chemistry Group (CATCO)
Department of Chemistry
Southern Methodist University
3215 Daniel Ave, Dallas, Texas 75275-0314 (USA)

Supporting information for this article is available on the WWW under https://doi.org/10.1002/cplu.202100285

This article is part of a Special Collection dedicated to the 4th International Symposium on Halogen Bonding (ISXB-4).

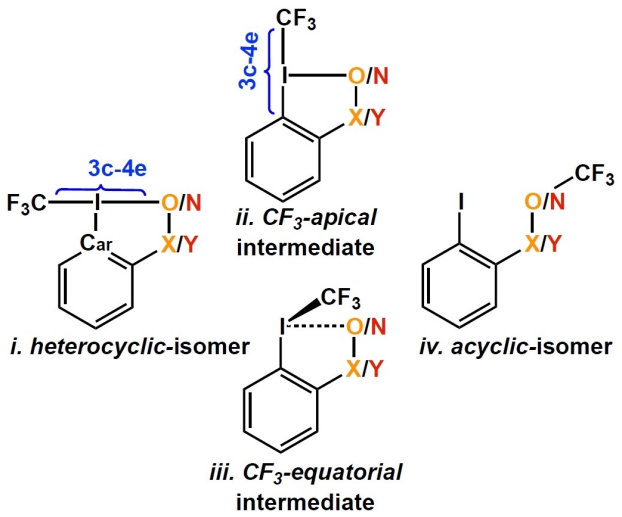

Figure 1. Different conformations considered in this work. C_{ar} identifies the carbon of the aromatic ring to distinguish between different types of C–I bonds. Molecules containing O–X linker (in orange) represent group 1, whereas N=Y linker (in red) represent group 2 molecules.

stabilize the compounds.[18] The geometry around the trivalent iodine is T-shaped, as predicted by valence-shell electron-pair repulsion (VSEPR) theory,[19] with the iodine two lone pairs occupying equatorial positions to minimize mutual repulsion between electron pairs.[16a]

The higher reactivity of the axial bonds in these systems and the tendency of electronegative ligands to occupy axial positions are easily understood in terms of Musher molecular orbital model.[11] According to this model the axial ligands are bound to iodine via a 3c–4e bond,[20] made from the linear combination of three σ-oriented valence p-orbitals located at each atomic center and populated by four electrons, leading to occupied bonding and non-bonding orbitals and an empty anti-bonding orbital. Both axial bonds are electron deficient, having a fractional bond order, which is in line with their higher reactivity. The occupied non-bonding orbital is centered at the ligands with a node at iodine indicating that the electron density is polarized toward the axial ligands, hence electronegative atoms are expected to stabilize 3c–4e bonds. This is also supported by orbital localization methods, showing that 3c–4e bonds can be seen as two highly polar 2c–2e bonds.[21] According to valence bond (VB) theory, 3c–4e bond molecular orbitals can be related to a set of ionic-covalent valence bond resonance structures,[22] e.g., for XeF_2 two partially ionic partially covalent resonance structures (FXe^+ F^- and F^- XeF^+) contribute mostly to the electronic structure. The VB charge-shift bond model suggests that 3c–4e bonds are not stable because of individual VB structures but because of the resonance between ionic-covalent VB structures,[23] indicating the confluence of covalent and ionic contributions to 3c–4e bonding.[24] Common to the different VB and MO models is the synergy of both covalent and ionic contributions to the stability of 3c–4e bonding. It is worth mentioning that 3c–4e bonds and XBs are closely related.[8] As the bond strength and the covalent character of XB increase, we observe a smooth transition to 3c–4e bonding.[2a,7a,25]

Experimental and theoretical studies have shown that electronegative ligands in a trans position to each other do not guarantee the stability of Togni-like reagents or other aryl-λ^3-Iodanes. Mutual influence of the ligands in 3c–4e bonding, also called trans influence, does also play an essential role in the thermodynamic stability of these compounds. Ochiai and co-workers[26] utilized bond distances taken from X-ray diffraction data, to rank the trans influence of a series of ligands according to their elongating effect on a given trans ligand bond. Based on a systematic series of isodesmic ligand exchange reaction energies, they concluded that greater stability is obtained by combining a ligand with large trans influence with one with small trans influence or by choosing two moderately trans influence ligands.

Sajith and Suresh[27] tested the relationship between bond distances and several electronic parameters and found a linear correlation for the density at the bond critical point (BCP) and the minimum electrostatic potential. They also derived an empirical equation based solely on these parameters to predict bond dissociation energies (BDE), showing the importance of the trans influence for variations in the BDE values.

The heterolytic I–CF_3 bond dissociation energy is a useful parameter to rank the trifluoromethyl cation-donating ability (TCDA) of Togni-like reagents.[28] Xue, Cheng, and co-workers[28] created a TCDA scale based on heterolytic bond dissociation enthalpies of more than 99 electrophilic reagents, including several Togni-like compounds. They found a good TCDA correlation based on experimental data of popular reagents. Schaefer and coworkers[29] followed a similar strategy and found that by modifying the linker X group in Togni I reagents from $X=C(CH_3)_2$ to $X=SO_2$ (see Figure 1) there is a significant decrease in the heterolytic dissociation free energy. Utilizing this modified reagent for the zinc-mediated trifluoromethylation of 1-pentanol resulted in a free-energy barrier of 8.1 kcal/mol, which is smaller than that predicted for the original Togni I reagent.

Worth mentioning is that hypervalent iodine reagents are usually energetic materials that need to be handle with care. Recently, Kraka and coworkers investigated the infrared spectra of benziodazolotetrazoles and benziodoxoles,[30] using the local vibrational mode analysis[31] as an efficient tool for the decomposition of delocalized normal modes into local mode contributions related to bonds stretching, bending or torsion, providing a facile chemical interpretation and a quantitative measure of bond strength derived from the associated local stretching force constants. They could associate the explosive decomposition of benziodazolotetrazoles to the weak I–N bonds of these compounds, whereas their benziodoxole counterparts were found to be more stable due to their stronger I–O bonds.[30] Togni reagents are not highly reactive per se, but could become sensitive and therefore, should not be heated vigorously to avoid any risk of a possible explosion.[16a]

Togni reagents isomerization can occur via two different pathways.[32] The CF_3 group can move to an apical position (see conformation ii in Figure 1), resulting in an intermediate where

the 3c–4e bond changes from C–I–O to C–I–C_{ar} (C_{ar} denotes the carbon at the aromatic ring), or to an equatorial position (see conformation iii in Figure 1), where C–I–C_{ar} has an angle of about 90 degrees and no 3c–4e bond is expected. In either of the two pathways, the transfer of CF_3 from iodine to oxygen is the higher energy barrier step.

Recently, the Togni group developed a new reagent (HYPISUL),[17,18] which we will call Togni III in the following. The main difference of this reagent is the use of a sulfoximine linker, in which an sp^2 nitrogen is involved in the 3c–4e bond with iodine. Togni III is especially suitable for the trifluoromethylation of aliphatic alcohols, affording the corresponding ethers in moderate to high yield.[17] As commonly observed for Togni reagents an activation by an acid catalyst is required.[16a,17,33]

In view of the current open questions regarding the relationship between trans influence and 3c–4e bonding and to shed more light on the unusual structure of the stable intermediate found in the second path of the isomerization reaction mechanism (conformation iii in Figure 1), we investigated the strength and nature of iodine bonding in a set of 32 Togni-like reagents chosen based on previous studies,[16a,17,29,32] and complemented by a systematic modification of the linker and its substituents. Instead of relying on structural parameters, such as bond distances, which have a lower sensitivity to changes in the electronic structure and as such to the trans influence, we used a highly sensitive bond strength measure derived from vibrational spectroscopy. As a complement we used energy and electron density-based properties to address the following questions:

1. Can we explain the thermodynamic stability of the different conformations adopted by Togni-like reagents based on a bond strength analysis?
2. Can we relate the charge-shift character of hypervalent iodine bonds to their strength and nature?
3. Can we single out the major electronic effects that play a key role in the trans influence?
4. Which types of linkers provide a wider range of TCDA to Togni-like reagents, the ones where iodine is bonded to a sp^2 nitrogen (represented by N and Y in Figure 1), as found in Togni III, or to a sp^3 oxygen (represented by O and X in Figure 1), as found in Togni I and II reagents?

Results and Discussion

Our series of 32 Togni-like reagents were separated into two groups according to the nature of the atom connected to iodine. Group one are molecules with linkers connecting the aromatic ring to iodine via an sp^3 oxygen (molecules **1.1**–**1.17**), such as Togni I (molecule **1.1**) and II reagents (molecule **1.4**), whereas group two are reagents with linkers connected to iodine via an sp^2 nitrogen (molecules **2.1**–**2.15**), such as Togni III (**2.14**). Substituents at the linker were modified in a systematic fashion. The geometries of all reagents were fully optimized in acetonitrile for each of the four different conformations shown in Figure 1. Conformation i is the cyclic-isomer, where CF_3 is trans to the most electronegative ligand (O for group one and N for group two), conformation ii has the CF_3 moved to an apical position, where CF_3 is trans to C_{ar}, i.e., the carbon of the aromatic ring, conformation iii results from the rotation of the CF_3 into an equatorial position, and conformation iv is an acyclic-isomer, where CF_3 is transferred to O or N.

Figure 2 shows all molecules considered in the present study in their cyclic isomer conformation i with color-coded group NBO charges obtained in acetonitrile solution (individual atomic charges and group charges for all other conformations can be found in tables S1 and Figures S1–S3 of the SI). The cyclic-isomer (conformation i in Figure 1) is characterized by an iodine with a T-shaped geometry, where the 3c–4e bond is quasi-linear, with C–I–O/N angles varying from 168 to 179°, and planar or quasi-planar dihedral C–I–C_{ar}–O/N angles varying from 178 to 180°). The two iodine ligands are not necessarily co-planar to the phenyl ring, the torsion between these ligands and the phenyl ring can be as much as 21° (molecule **1.7**). The apical-CF_3-conformation, ii in Figure 1, where the 3c–4e bond is moved to C–I–C_{ar} has also a T-shaped geometry around iodine. However, the C–I–C_{ar} angle shows a higher deviation from linearity, varying from 138 to 166°. The equatorial-CF_3-conformation (conformation iii in Figure 1) has an even more bent C–I–C_{ar} angle precluding the formation of a 3c–4e bond, and a long I–O/N contact of about 3.0 Å, suggesting an unusual divalent iodine, covalently bonded only to the carbons and forming a long and weak attractive interaction with the O/N atom of the linker group. A local minimum with CF_3 in apical position (conformation ii) was found for most molecules, exceptions being **1.11** and **1.14**–**1.17** where just a local minimum with CF_3 in the equatorial position (conformation iii) was found. For several molecules **1.4**, **1.5**, **1.9**, **1.10**, **1.12**, **1.13**, **2.4**, **2.5**, **2.8**, **2.9**, **2.12**–**2.15** both minima were found.

In the acyclic isomer (conformation iv) the CF_3 group is transferred to O (**1.1**–**1.17**) or N (**2.1**–**1.15**). In this conformation, the I–O/N distance varies from 3.1 to 4.6 Å depending on the torsion of the linker and is at least 0.22 Å longer than the I–O/N interaction found in conformation iii. No 3c–4e bond was observed and the iodine is monovalent.

Charge distribution. ELF provides a measure of electron localization, being useful to visualize electron pair domains such as lone-pairs and π-bonds. In Figure 3 we provide ELF plots utilizing an isodensity value of 0.85 to show the lone-pair domains at the iodine for conformations i-iv for Togni II (**1.4**). In conformations i and ii we see a similar pattern, i.e., the molecules have a T-shaped geometry with two lone pairs at an equatorial position (approximately perpendicular to the plane formed by I and its three ligands). In conformation iii the lone pairs are further apart, and one lone pair is positioned between I and O indicating a divalent iodine situation, typical of an iodonium,[34] suggesting an ion-pair structure with a positively charged iodine (NBO (I): 0.81e) and a negative charge delocalized over the CO_2 linker (NBO (CO_2): −0.78e). In conformation iv a belt-shaped region is formed around iodine, common to monovalent iodine.[35] Figure 3 also shows the anisotropic charge distribution for Togni II (molecule **1.4**) via molecular electrostatic potentials mapped onto the 0.001e/$bohr^3$ isodensity (representing the van der Waals surface).[36] In

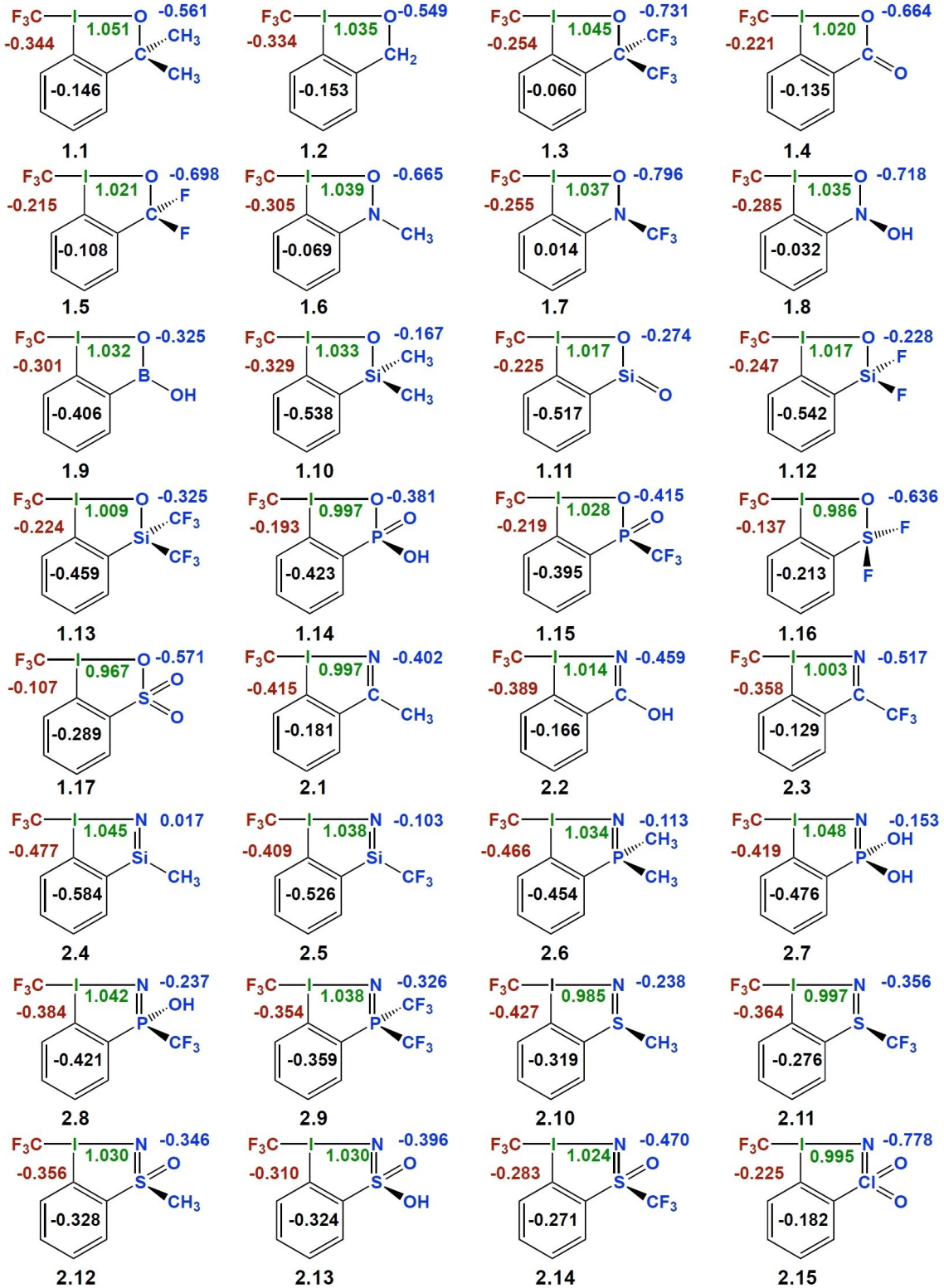

Figure 2. Togni-like reagents studied in this work given in their cyclic-isomer conformation i. NBO charges (units in [e]) obtained in acetonitrile solution for the iodine atom are shown in green color, in red color NBO group charges are given for the CF_3 ligand and in blue color for the opposite ligand. M06-2X/Def2-TZVP (D for I) level of theory.

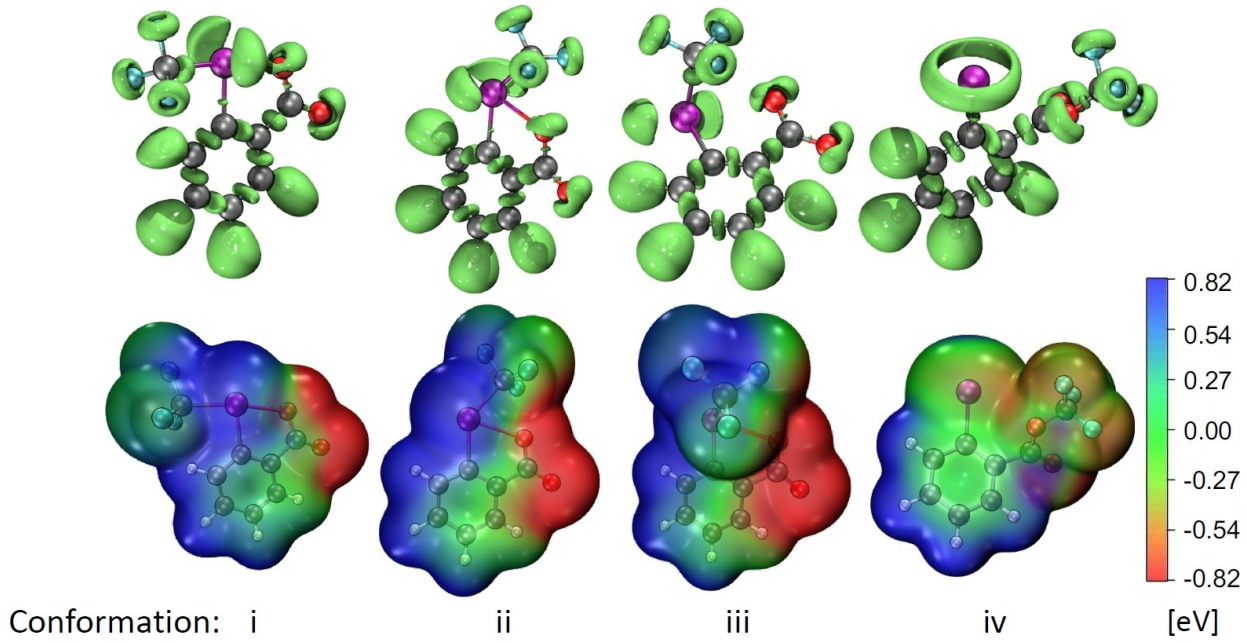

Figure 3. Electron localization function plotted at an isodensity value of 0.85 to visualize the lone pair positions (upper part) and the molecular electrostatic potential (lower part) showing the anisotropic charge distribution for conformations i–iv. M06-2X/Def2-TZVP (D for I) level of theory.

conformations i–iii the linkers are the most negatively charged part of the molecules whereas iodine is positively charged. The transfer of the CF_3 group from iodine to oxygen results in a decrease of charge separation between iodine and the linker atoms, i.e., this conformation has less polar bonds.

Bond strength and bond length. The bond strength analysis was based on local stretching force constants k^a derived from local vibrational modes originally introduced by Konkoli and Cremer[37] and recently described in a comprehensive review article.[31] These local vibrational modes have the advantage of being free from any mode-mode coupling encountered in normal vibrational modes.[38] Therefore, the associated local stretching force constants k^a provide a reliable and unique measure of the intrinsic strength of a chemical bond or weak chemical interaction[39] which has been extensively applied in previous work as documented in Ref.[31] For some more recent work see also Refs. [40] Bond length is commonly associated with bond strength. However, a caveat is appropriate; under certain circumstances, a shorter bond is not necessarily a stronger bond, as reported in the literature.[40f,41] Figure 4 shows the relationship between bond length and the intrinsic strength of the iodine bonds as reflected by k^a for conformations i–iii. Previous studies on C–X (X = halogens, chalcogens, pnicogens, and H) bonds[42] of a large set of different systems showed that a close to exponential decay relating k^a and r is commonly observed for each bond type. In the case of X substituents of the same period of the periodic table, a single curve may still be suitable, due to the similar effective core size of these substituents. In the present study, a single exponential curve fits well for all I–O and I–N bonds in conformation i, ii, and iii (red curve in Figure 4). Unexpectedly, two independent curves, are found for the I–C bonds, one for the I–C bond involving the CF_3 group and the other for the bond involving the aromatic ring (I–C_{ar}). This can be partially attributed to the different chemical environment of the C atoms; in CF_3, carbon is positively charged due to the three electronegative fluorine substituents, whereas the aryl ring carbon is negatively charged (see NBO atomic charges in table S1 of the SI), partially attributed to the different nature of that I–C bonds. In conformation i, the I–C bond is part of the 3c–4e bond, having a high charge-shift character, whereas the I–C_{ar} is closer to a 2c–2e classical bond. In conformation ii, both I–C and I–C_{ar} bonds are part of the 3c–4e bond and have similar characteristics resulting in closer but still separated curves. In conformation iii, even though I–C and I–C_{ar} are both of covalent nature, they do not fit into a single curve due to the different chemical environment of the carbon atoms.

Bond nature. To probe the nature of the iodine bonds and their relation to bond strength in more detail, the electron density ρ_b, its Laplacian $\nabla^2\rho_b$, and the energy density H_b computed at the bond critical point (BCP) were analyzed. According to the Cremer-Kraka criterion,[43] a covalent bond is characterized by the presence of an electron density path connecting the bonded atoms (necessary condition) and a stabilizing, thus negative, energy density at the BCP ($H_b < 0$; sufficient condition). Figure 5 shows the correlation between bond strength given by k^a values and the covalent character of the iodine bonds given by H_b values for conformation i–iii (numerical values are compiled in Tables S2–S7 in the SI). As the bonds become more covalent, they tend to be stronger. For conformation i the relationship is linear, a single line fits relatively well for the different types of bonds ($R^2 = 0.950$). As expected from Musher's hypervalent model, the I–C and I–O/N bonds involved in 3c–4e bonding tend to be less covalent than

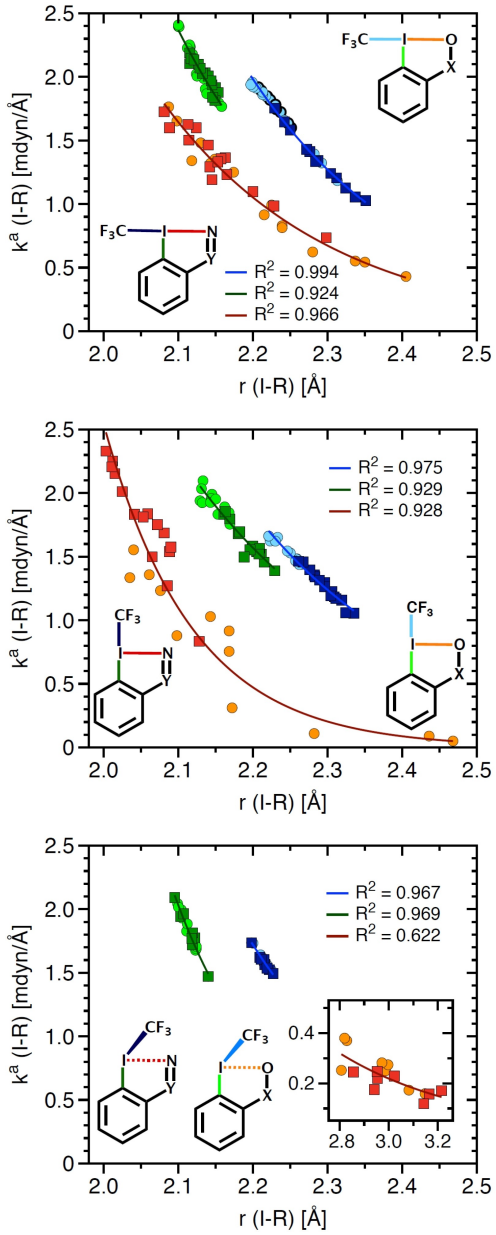

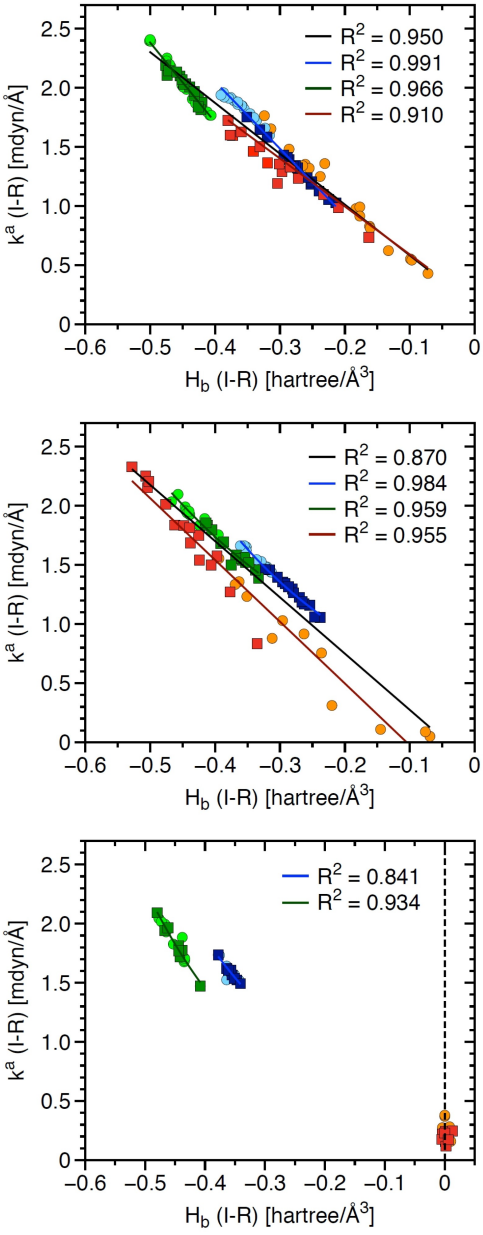

Figure 4. Exponential bond strength-bond length relationships involving I–R bonds (R = C, N or O) for conformations i, ii and iii on top, middle and bottom respectively. Square markers and darker colors for bonds in 1.1–1.17, light colors and circles for 2.1–2.15, orange color for I–O, red color for I–N, blue color for I–CF_3 and green color for I–C_{ar} bonds. M06-2X/Def2-TZVP (D for I) level of theory.

Figure 5. Correlation between k^a and the energy density H_b for conformations I, ii and iii, on top, middle and bottom respectively. The same color code was used as for Figure 4. M06-2X/Def2-TZVP (D for I) level of theory.

the I–C_{ar} bonds. Conformation ii does also show a linear correlation between k^a and H_b, however, a single linear fit provides a much lower correlation $R^2 = 0.870$ compared to individual fits for each bond type ($R^2 = 0.955$–0.984). In this conformation, the I–O bonds (in **1.1**–**1.17**) tend to be weaker and less covalent than the I–N bonds (in **2.1**–**2.15**) and the I–O/N interactions are not necessarily stronger than the bonds I–C and I–C_{ar} involved in the 3c–4e bond. In conformation iii, we clearly see that I–O/N are very weak non-covalent interactions, whereas I–C and I–C_{ar} are strong and covalent bonds, confirming iodine as divalent in conformation iii, i.e., covalent I–O/N bonds are not formed.

Bader and Essén[44] utilized ρ_b and $\nabla^2\rho_b$ to distinguish between shared-shell interactions and closed-shell interactions. The former is characterized by large ρ_b and negative $\nabla^2\rho_b$ values indicating local charge concentration, typical of a covalent bond, whereas the latter is characterized by relatively small ρ_b and positive $\nabla^2\rho_b$ values due to local charge depletion, typical of van der Waals and ionic interactions. Shaik and co-workers[45] complemented this analysis by pointing out that a common signature of a charge-shift bond is an electron density comparable to those found for covalent bonds accompanied by a positive or close to zero Laplacian value. Charge-shift bonds

usually occur between two lone-pairs-rich atoms such as halogens and chalcogens, 3c–4e bonds, and confined atoms, where the positive sign of the Laplacian is attributed to a local excess of kinetic-energy due to exchange-repulsion.[46]

The relationship between ρ_b and $\nabla^2\rho_b$ is shown in Figure 6 for all I–R (R = C, N, O) bonds of conformations i, ii and iii, respectively. In conformation i the 3c–4e bonds formed by I–O, I–N, and I–C (shown in orange, red, and blue color in Figure 6) can be considered as charge-shift bonds, with relatively large ρ_b values and positive or close to zero $\nabla^2\rho_b$ values, whereas the

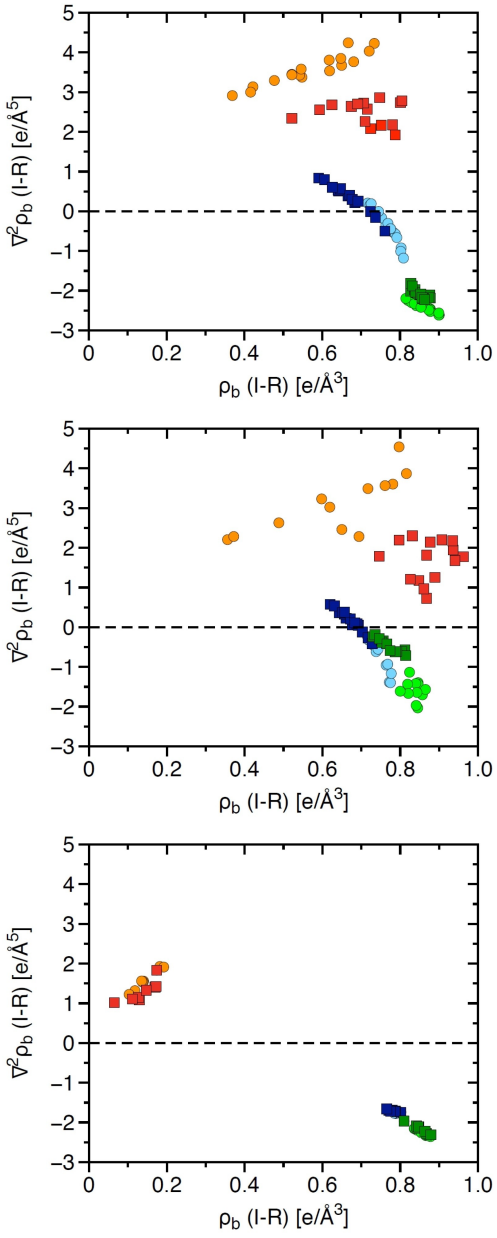

Figure 6. Relationship between ρ_b and $\nabla^2\rho_b$ of the I–R bonds (R = C, N or O) for conformations i, ii and iii, on top, middle and bottom respectively. The same color code was used as for Figure 4. M06-2X/Def2-TZVP (D for I) level of theory.

I–C_{ar} bonds (in green) are clearly shared shell interactions (i.e., covalent bonds) due to their larger ρ_b and negative $\nabla^2\rho_b$ values. As ρ_b increases, two opposite trends are observed for $\nabla^2\rho_b$ of I–C and I–O/N bonds. For the I–C bonds, $\nabla^2\rho_b$ values decrease, approaching the I–C_{ar} covalent bond values, whereas for IO/N the $\nabla^2\rho_b$ values increase suggesting an increase in charge-shift character, which is especially more accentuated for the more electronegative, lone-pair-rich O compared to N. The different behavior is in accordance with the fact that electronegative atoms such as F and O have a greater tendency to form charge-shift bonds than carbon.[46] Noteworthy is that as ρ_b increases, H_b and k^a do also tend to increase for both I–C and I–O/N bonds (see Figure S5 and S6 in the SI).

Moving CF_3 to the apical position (conformation ii), leads to an increase in $\nabla^2\rho_b$ of the I–C_{ar} bonds, changing their character from covalent to charge-shift (especially noticeable for **2.2**–**2.15** shown in dark green) as this bond starts to contribute to the 3c–4e bond. However, the I–O/N bond, which is not part of the 3c–4e bond in conformation ii, has still the charge-shift signature due to the high electronegativity of O and N. As ρ_b values increase, $\nabla^2\rho_b$ values do also increase for most I–O bonds. Although no clear trend is observed for the I–N bonds, $\nabla^2\rho_b$ values are less positive than the ones found in conformation i, indicating that outside the 3c–4e bond the I–N bond has a lower charge-shift character. Moving CF_3 to an equatorial position (conformation iii), results in I–O/N bond of non-covalent character (small ρ_b and positive $\nabla^2\rho_b$ values) and I–C and I–C_{ar} bonds of covalent character (large ρ_b and negative $\nabla^2\rho_b$ values), in consonance with the k^a versus H_b analysis.

The stability of Togni-like reagents in their kinetically stable conformation i can be fine-tuned by maximizing the charge-shift character of the I–O bond and to a lesser extent that of the I–N bond, leading to stronger, hence less reactive 3c–4e bonds (see Figure S6 for k^a versus $\nabla^2\rho_b$). Conversely, the reactivity of these compounds can be fine-tuned by weakening the I–O or I–N bond.[34,47] In this case, substituents at the linker capable of reducing I–O or I–N charge-shift character will improve the reactivity of the reagent.

Bond strength and thermodynamic stability. For all systems studied, the acyclic isomer (conformation iv) was found to be thermodynamically more stable than conformation i (numerical values are compiled in Table S8 of the SI). However, computational studies have shown that the isomerization to the acyclic conformation is not observed due to the high energy barrier of this reaction.[48] Conformations ii and iii are of higher energy than conformation i and can be considered as possible intermediates of the isomerization of i into iv.[32,47b] The greater stability of the acyclic conformation iv can be easily rationalized and understood on the basis of our bond strength analysis. The stronger O–C **1.1**–**1.17** or N–C **2.1**–**2.15** bond formed in the acyclic isomer has a k^a value varying from 4.711 mdyn/Å (for **2.3**) to 6.502 mdyn/Å (for **1.10**), a value which is larger than that found for the individual I–C and I–O/N bonds and also larger than the sum of the k^a values of the 3c–4e bonds reaching at most 4.213 mdyn/Å. Consequently, the acyclic isomer is also less reactive and is not suitable for CF_3 group transfer. The greater stability of conformation i compared

to ii and iii can also be understood on the basis of bond strength differences. However, these are more subtle and require the evaluation of all iodine contacts.

Comparing the bond strength of molecules **1.1**–**1.17** in conformations i and ii, conformation ii has overall weaker I–C, I–C_{ar}, and I–O bonds than conformation i. The weaker I–C and I–C_{ar} bonds are due to the lower electronegativity of C_{ar} compared to O rendering a less stable 3c–4e bond compared to the ones found for conformation i, whereas the weaker I–O bonds in conformation ii indicate that this bond is better stabilized by being part of the 3c–4e bond, where it can retain a higher charge-shift character. As a consequence of these weakened bonds, conformation ii is 11.1–22.6 kcal/mol less stable than conformation i (see Table S8 of the SI). Molecules **1.14**–**1.17** have the weakest I–O bonds in conformation i and are no longer found to be stable in conformation ii.

Molecules of group 2 (**2.1**–**2.15**) have also weaker I–C and I–C_{ar} bonds in conformation ii due to less stable 3c–4e bonding, but different from the I–O bonds in group 1 (**1.1**–**1.17**), the I–N bonds in conformation ii are slightly stronger than in conformation i, indicating that charge-shift plays a lesser stabilizing role and covalent contributions a higher role for I–N bonds. For molecules of group 2, the energetic differences between conformation i and ii are in general smaller, varying from 3.3 to 17.6 kcal/mol. Conformation iii tends to be less stable than i and ii, exceptions in which iii is more stable than ii are molecules possessing very weak I–O or I–N bonds in conformation ii as in **1.4**, **1.5**, **1.12**–**1.17**, and **2.15**.

Trans influence and I–O/N bond strength. According to what is known as trans influence, the weakening of the I–O/N bond in conformation i is usually accompanied by the strengthening of the I–C bond trans to it. Figure 7 shows that the trans influence involves two different linear trends. A steeper one for **2.1**–**2.15** molecules is characterized by having a I–N bond and a less steep one for molecules that possess an I–O bond (**1.1**–**1.17**), indicating that the I–C bonds in the former are more sensitive to changes in the linker. This is reflected by the atomic charges, which vary from −0.71 to −1.51e for nitrogen in molecules **2.1**–**2.15** but have a smaller range of −0.69 to −1.29e for oxygen (see O and N atomic charges in Table S1) in **1.1**–**1.17**. Opposite trends of the I–O/N and I–C bond strengths are accompanied by differences in their bonding nature. An increase in charge-shift given by $\nabla^2\rho_b$ or covalent character given by H_b of the I–O/N bond is accompanied by a decrease in the I–C bonds (see Figures S7 and S8 of the SI). Prominent outliers in Figure 7 such as **1.10**, **1.3**, **2.4**, and **2.5** can be explained on the basis of the polarizing power of the linker. For example, molecule **1.10** has the least polarizing linker of group 1 (NBO: −0.167e; Figure 2) due to the combination of electropositive Si and methyl substituents. As a consequence, the CF_3 group has the lowest charge (−0.329e) and the I–C bond highest charge-shift character ($\nabla^2\rho_b = 0.190$ e/bohr^5). Replacing the methyl substituents by electron-withdrawing groups such as sp^2(O) in **1.11** or F atoms in **1.12** polarizes the negative charge at the CF_3 group toward the linker decreasing the charge-shift character of the I–C bonds ($\nabla^2\rho_b = -0.443$ (1.11); −0.304 (1.12) e/bohr^5) and leading to stronger I–C bonds (k^a(I–C) = 1.659 (**1.10**); 1.860 (**1.11**); 1.850 (**1.12**) mdyn/Å). On the other hand, C and N-based linkers with electron-withdrawing substituents in **1.3**–**1.5** and **1.7** strongly polarize the charge of CF_3, leading to stronger I–C bonds than expected from the linear fit. Deviations for group 2 molecules can be explained in similar terms. Molecules **2.5** and **2.9** have I–N bonds of similar strength (k^a(I–N) = 1.191(**2.5**); 1.233(**2.9**) mdyn/Å), but the I–C bond in the former is weaker (k^a(I–C) = 1.205(**2.5**); 1.413(**2.9**) mdyn/Å) due to the lower polarizing power of NSi(CF_3) compared to the NP(CF_3)$_2$ linker.

The polarizing power of the linker can also be accessed from the maximum electrostatic potential at the CF_3 carbon σ-hole region collinear to the I–C bond (V_{max}). A larger V_{max} indicates that electron density is more polarized toward the iodine. An increase in V_{max} is accompanied by an increase in (C–I) bond strength (see Figure S9) due to the electron density increase in the interatomic region and by a weakening of I–O/N bond (shown in Figure S10) due to exchange-repulsion pushing electrons from this bond towards O or N atoms.

Bond strength orders. Local vibrational force constants k^a can be transformed into relative bond strength orders (BSO), which are easier to interpret and to compare (e.g., see Refs. [39]), following the generalized Badger rule,[42a] in which bond strength orders are related to k^a via a power equation of the type:

$$\text{BSO } n = a(k^a)^b \tag{1}$$

The constants a and b in Eq. 1 are obtained from k^a values of two bonds of suitable reference compounds ($k^a{}_1$ and $k^a{}_2$) and assuming that their *BSO* n values (n_1 and n_2) equate to their known bond order and that *BSO* $n = 0$ for $k^a = 0$, resulting in Eqs. 2 and 3:

$$a = n_2(k^a{}_2)^b \tag{2}$$

$$b = ln(n_2/n_1)/ln(k^a{}_2/k^a{}_1) \tag{3}$$

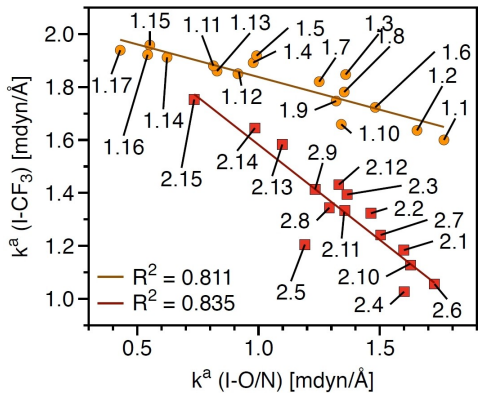

Figure 7. Inverse correlation between the strength of I–CF3 and I–O (red squares) I–N (orange circles) bonds as reflected by their k^a values, shown for conformation i. M06-2X/Def2-TZVP (D for I) level of theory.

In the present study we took as the first reference the I–O single bond in HO–I ($n_1 = 1.0$; $k^a{}_1 = 3.380$ mdyn/Å) and the 3c–4e bond in $(HO–I–OH)^-$ anion as the second reference ($n_2 = 0.5$; $k^a{}_2 = 1.348$ mdyn/Å), resulting in $a = 0.399$ and $b = 0.754$. For a consistent description, reference k^a values were obtained at the same level of theory and the same solvent model utilized for the Togni-like molecules. The choice of the references was supported by Wiberg bond indexes[49] of a similar 2:1 ratio (0.86 for O–I bond in HOI and 0.48 for $IO_2H_2^-$).

Bond strength and dissociation energies. The C–I heterolytic bond dissociation disrupts the 3c–4e bond leading to the formation of CF_3^+ and a monovalent iodine anion which can be stabilized by a Lewis or Brønsted acid.[16a,33] The linear correlation between I–O/N bond strength and the heterolytic bond dissociation energy (BDE) shown in Figure 8, indicates that the energetic cost of the dissociation process is mostly determined by the strength of the I–O/N bond. The key role of I–O/N bond is also confirmed by the high linear correlation between BDE and the energy related to breaking I–O/N by the rotation of CF_3 group given by the difference between conformation i and iii shown in Figure S11. Weakening of this bond should lead to lower BDE values and facile trifluoromethylation of a target molecule. Schaefer and co-workers[29] have previously utilized this idea in conjunction with a non-ideal bond length-bond strength relationship and identified molecule **1.17** as a possible candidate for a new Togni-like reagent due to its long, thus weak I–O bond. Besides the limitations of the bond-strength bond length relationship already discussed, BSO provides a better exponential correlation with the BDE, as shown in Figure 8 ($R^2 = 0.963$ *vs.* 0.909 for bond length). In the following, we provide a detailed analysis of how the linker may affect the strength of I–O bond in molecules **1.1**–**1.17** and the I–N bond in molecules **2.1**–**2.15**; a valuable information for the synthesis of more reactive trifluoromethylating Togni reagents.

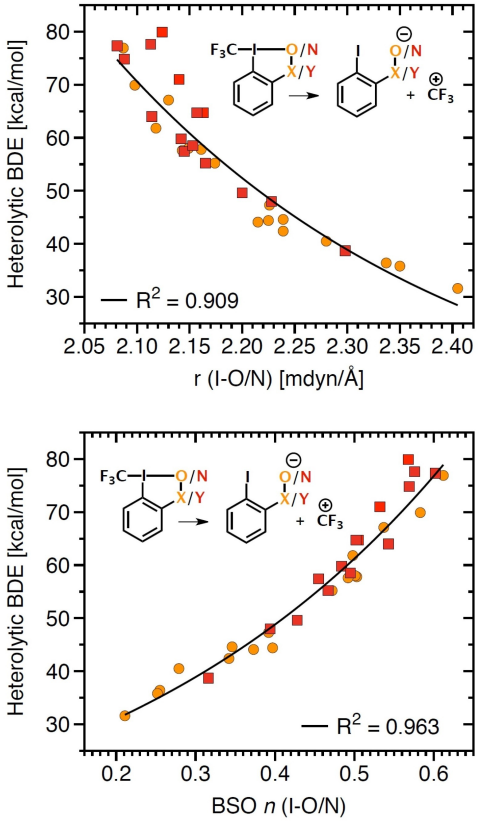

Figure 8. Trans influence as reflected by the correlation of the heterolytic bond dissociation energy and the I–O/N bond distance (upper part) and between the heterolytic bond dissociation energy and the bond strength given by k^a I–O/N. M06-2X/Def2-TZVP (D for I) level of theory.

Starting from Togni reagent **1.1** and changing the methyl substituents at the carbon atom of the linker molecules **1.2**–**1.5** are obtained. In this series, the BSO of the I–O bond decreases from 0.612 (**1.1**) to 0.397 (**1.5**) (Table S2) and the BDE from 76.9 to 44.4 kcal/mol (Table S9) as the electron-withdrawing nature of the substituent increases ($CH_3 < H < CF_3 < sp^2(O) \approx F$). We found that replacing the carbon of the linker with the more electronegative nitrogen results in a weaker I–O bond (BSO: 0.537–0.472) and lower BDE values (67.1–55.2 kcal/mol) which are more pronounced for the methylated systems (**1.1** compared to **1.6**), but of similar magnitude for the trifluorinated systems (**1.3** compared to **1.7**).

Replacing the N in **1.8** with the less electronegative B leads to **1.9**; a molecule that possesses a more negatively charged oxygen atom (NBO (O): −0.711 (**1.8**) and −1.008 (**1.9**)) and aromatic ring (NBO (O): −0.032 (**1.8**) and −0.406 (**1.9**)). Interestingly, BSO and BDE values are similar for **1.8** and **1.9**, (BSO: 0.501 (**1.8**); 0.492 mdyn/Å (**1.9**) and BDE: 58.0 and 57.6 kcal/mol, respectively), the largest difference being the weaker I–C_{ar} bond in **1.9**. Introducing a second-row atom such as Si, P, S at the linker results in a more expressive weakening of the I–O bond. Comparing e.g., molecules **1.10** and **1.13** which are the silicon analogs of **1.1** and **1.3**, there is a decrease of about 0.100 in BSO accompanied by a decrease of about 15 kcal/mol in BDE. Hypervalent S and P compounds result in even smaller BSO and BDE values, due to the presence of extra electron-withdrawing substituents. The lowest values were observed for **1.17**, (BSO: 0.430; BDE: 31.6 kcal/mol), i.e., the molecule which was recently proposed by Schaefer and co-workers.[29]

We also found similar trends for molecules based on the Togni III reagent (**2.1**–**2.15**), i.e., electron-withdrawing substituents at the carbon of the linker makes the I–N bond weaker and replacing carbons by third-row atoms such as Si, P, S, and Cl, leads to a further weakening of the I–N bond. However, the I–N bond strength given by k^a values and the BDEs are less sensitive to changes in the linker. Comparing e.g., molecules **2.6**, **2.9**, **2.13**, **2.14**, and **2.15** with the isoelectronic molecules **1.10**, **1.13**, **1.14**, **1.15**, and **1.17**, respectively we observe that the I–N bonds tend to be stronger than the I–O bonds.

Conclusion

In this work, we investigated the strength and nature of the bonds involving iodine for a set of 32 hypervalent iodine molecules based on Togni I, II (molecules **1.1**–**1.17**) and Togni III reagents (molecules **2.1**–**2.15**). The intrinsic strength of the iodine bonds was accessed with the help of local stretching force constants k^a and associated bond strength order values (BSO) derived from vibrational spectroscopy, whereas the nature of the bonds was obtained by an analysis of the energy density H_b, electron density ρ_b and the Laplacian $\nabla^2\rho_b$ at the BCP, complemented by ELF, MESP and NBO charge analyses. These bond properties were utilized to rationalize the main factors being responsible for the stability of these 32 molecules in four different conformations. We also investigated the trans influence with the help of k^a and BSO values and related the strength of the I–O or I–N bond to the heterolytic bond dissociation energies BDE. Our main conclusions resulting from this work are:

1. The non-reactive acyclic conformation iv is clearly more stable due to the O–C or N–C bonds formed which are much stronger than the 3c–4e bonds of the cyclic conformations. The stability of the three different cyclic conformations i–iii depends on all iodine bonds. For conformations i and ii a less electronegative atom (C < N < O) at the equatorial position (approximately orthogonal to the 3c–4e bond) is able to form a stronger and more covalent bond, whereas the 3c–4e bonds are better stabilized by the electronegative atoms O and N due to their capability of stabilizing charge-shift bonds like 3c–4e bonds.
2. Charge-shift bonds characterized by a large ρ_b value and a positive or close to zero $\nabla^2\rho_b$ behave differently according to the electronegativity of the atom involved. As the C–I bond becomes stronger $\nabla^2\rho_b$ decreases, whereas the opposite trend is found for O–I bonds. This is in line with the higher tendency of electronegative elements F and O to form charge-shift bonds.
3. Electron withdrawing substituents tend to weaken the I–O or I–N bond decreasing the heterolytic bond dissociation energies. Changing the linker atom connected to the aromatic ring from C with heavier elements such as Si, S, P can magnify this effect, especially hypervalent S and P compounds are capable of hosting extra electron-withdrawing substituents.
4. As the I–N or I–O bond becomes weaker the I–C bond in trans position tends to become stronger. This tendency is more accentuated for molecules **2.1**–**2.15** containing I–N bonds than for molecules **1.1**–**1.17** with I–O bonds. Comparing isoelectronic molecules, lower heterolytic bond dissociation values are observed for **1.1**–**1.17** due to the I–O bonds being weaker than I–N bonds.

A recent study[30] utilizing local mode analysis provides new insights into why benziodazolotetrazoles are unstable and potentially explosive, whereas their benziodoxole counterparts are relatively stable. The different behavior was attributed to the weaker I–N bonds of the former compared to the stronger I–O bonds of the latter. This can be contrasted with the present study, where I–N and I–O have a similar range of k^a values (k^a(I–N) = 0.735–1.725 mdyn/Å) and I–O (k^a(I–O) = 0.430–1.764 mdyn/Å). The reason for the molecules of the present study being able of forming I–N bonds as strong as I–O bonds are due to their sp^2 hybridization and less electronegative ligands (C, Si, P, S, and Cl compared to the N in benziodazolotetrazoles) resulting in a negative charge at the N atom that can surpass that of the O atom, whereas the N atom in benziodazolotetrazoles has a much higher charge than the O atom in benziodoxoles. Future studies will focus on how different Lewis acids may influence the strength and nature of the 3c–4e bonds via interaction with the O or N atoms of Togni-like reagents to better understand their activation role.

Computational Methods

All calculations were carried out in acetonitrile solvent described with the Solvent Model Based on Density (SMD18).[50] For an optimal balance between computational cost and accuracy, the M06-2X[10,51] exchange functional was combined with the Def2-TZVP[52] basis set for all atoms, except iodine for which Def2-TZVPD[53] and its associated effective-core potential[54] was utilized to account for relativistic effects. This model chemistry was successfully employed in the study of the isomerization mechanism of Togni I and II reagents[32,55] and it is consistent with the SMD18 parameterizations.[50b] An ultra-fine grid and a tight geometry optimization criterium were utilized in all calculation. Harmonic frequencies were computed for all geometries, no imaginary frequency was found, characterizing all systems as minimum in the potential energy surface.

The bond strength analysis based on k^a and BSO values was complemented by NBO atomic charges derived from the NBO analysis,[56] electron localization functions (ELF),[57] molecular electrostatic potentials (MESP)[58] and the analysis of local features of the electronic density derived from Bader's quantum atoms in molecules theory.[59] The focus in this work was on the energy density and the electron density and its Laplacian obtained at the bond critical point of the bonds (denoted by H_b, ρ_b, and $\nabla^2\rho_b$, respectively). Geometry optimizations followed by frequency calculations were carried with Gaussian16.[60] NBO charges and Wiberg indexes were obtained from NBO6,[61] ELF and MESP were generated using Multiwfn[62] and graphically displayed with VMD;[63] the electron density analysis was performed with AIMALL[64] and for the local mode analysis, the LModeA package was used.[65]

Acknowledgements

This research was funded by Brazilian agencies São Paulo Research Foundation (FAPESP), grant numbers 2018/13673-7 and 2019/25105-6 and National Council for Scientific and Technological Development (CNPq), grant number 307136/2019-1 and by the National Science Foundation grant number CHE 1464906. The authors thank SMU for providing generous computational resources.

Conflict of Interest

The authors declare no conflict of interest.

Keywords: bond strength order · charge-shift · hypervalent iodine · local mode analysis · Togni reagents

[1] a) Z. Zhu, Z. Xu, W. Zhu, *J. Chem. Inf. Model.* **2020**, *60*, 2683–2696; b) P. R. Varadwaj, A. Varadwaj, H. M. Marques, *Inorganics* **2019**, *7*, 40; c) H. Yang, M. W. Wong, *Molecules* **2020**, *25*, 1045; d) G. Berger, P. Frangville, F. Meyer, *Chem. Commun.* **2020**, *56*, 4970–4981.
[2] a) V. Oliveira, D. Cremer, *Chem. Phys. Lett.* **2017**, *681*, 56–63; b) V. P. Oliveira, B. L. Marcial, F. B. C. Machado, E. Kraka, *Materials* **2020**, *13*, 55.
[3] G. Cavallo, P. Metrangolo, R. Milani, T. Pilati, A. Priimagi, G. Resnati, G. Terraneo, *Chem. Rev.* **2016**, *116*, 2478–2601.
[4] a) P. Politzer, J. S. Murray, T. Clark, in *Halogen Bonding I: Impact on Materials Chemistry and Life Sciences* (Eds.: P. Metrangolo, G. Resnati), Springer International Publishing, Cham, **2015**, pp. 19–42; b) T. Clark, M. Hennemann, J. S. Murray, P. Politzer, *J. Mol. Model.* **2007**, *13*, 291–296.
[5] E. Engelage, D. Reinhard, S. M. Huber, *Chem. Eur. J.* **2020**, *26*, 3843–3861.
[6] M. Freindorf, S. Yannacone, V. Oliveira, N. Verma, E. Kraka, *Crystals* **2021**, *11*, 373.
[7] a) V. Oliveira, E. Kraka, D. Cremer, *Phys. Chem. Chem. Phys.* **2016**, *18*, 33031–33046; b) V. Oliveira, E. Kraka, D. Cremer, *Inorg. Chem.* **2017**, *56*, 488–502.
[8] L. P. Wolters, P. Schyman, M. J. Pavan, W. L. Jorgensen, F. M. Bickelhaupt, S. Kozuch, *WIREs Comput. Mol. Sci.* **2014**, *4*, 523–540.
[9] J. K. Salunke, N. A. Durandin, T.-P. Ruoko, N. R. Candeias, P. Vivo, E. Vuorimaa-Laukkanen, T. Laaksonen, A. Priimagi, *Sci. Rep.* **2018**, *8*, 14431.
[10] S. Kozuch, J. M. L. Martin, *J. Chem. Theory Comput.* **2013**, *9*, 1918–1931.
[11] J. I. Musher, *Angew. Chem. Int. Ed. Engl.* **1969**, *8*, 54–68.
[12] a) M. C. Durrant, *Chem. Sci.* **2015**, *6*, 6614–6623; b) A. Kalemos, I. R. Ariyarathna, S. N. Khan, E. Miliordos, A. Mavridis, *Comput. Theor. Chem.* **2019**, *1153*, 65–74; c) R. H. Crabtree, *Chem. Soc. Rev.* **2017**, *46*, 1720–1729; d) S. Scheiner, J. Lu, *Chem. Eur. J.* **2018**, *24*, 8167–8177.
[13] A. Yoshimura, V. V. Zhdankin, *Chem. Rev.* **2016**, *116*, 3328–3435.
[14] F. C. Sousa de Silva, A. F. Tierno, S. E. Wengryniuk, *Molecules* **2017**, *22*, 780.
[15] X. Yang, T. Wu, R. J. Phipps, F. D. Toste, *Chem. Rev.* **2015**, *115*, 826–870.
[16] a) J. Charpentier, N. Früh, A. Togni, *Chem. Rev.* **2015**, *115*, 650–682; b) G. K. Murphy, T. Gulder, in *Fluorination* (Eds.: J. Hu, T. Umemoto), Springer Singapore, Singapore, **2018**, pp. 1–32; c) X. Shao, X. Wang, T. Yang, L. Lu, Q. Shen, *Angew. Chem. Int. Ed.* **2013**, *52*, 3457–3460; *Angew. Chem.* **2013**, *125*, 3541–3544; d) J. Schörgenhumer, M. Waser, *Org. Chem. Front.* **2016**, *3*, 1535–1540; e) S. Shu, Y. Li, J. Jiang, Z. Ke, Y. Liu, *J. Org. Chem.* **2019**, *84*, 458–462.
[17] J. Kalim, T. Duhail, E. Pietrasiak, E. Anselmi, E. Magnier, A. Togni, *Chem. Eur. J.* **2021**, *27*, 2638–2642.
[18] J. Kalim, T. Duhail, T.-N. Le, N. Vanthuyne, E. Anselmi, A. Togni, E. Magnier, *Chem. Sci.* **2019**, *10*, 10516–10523.
[19] R. J. Gillespie, *Coord. Chem. Rev.* **2008**, *252*, 1315–1327.
[20] a) G. C. Pimentel, *J. Chem. Phys.* **1951**, *19*, 446–448; b) R. E. Rundle, *J. Chem. Phys.* **1949**, *17*, 671–675.
[21] W. Kutzelnigg, *Angew. Chem. Int. Ed. Engl.* **1984**, *23*, 272–295.
[22] C. A. Coulson, *J. Chem. Soc.* **1964**, 1442–1454.
[23] B. Braïda, P. C. Hiberty, *Nat. Chem.* **2013**, *5*, 417–422.
[24] S. Shaik, D. Danovich, J. M. Galbraith, B. Braïda, W. Wu, P. C. Hiberty, *Angew. Chem. Int. Ed.* **2020**, *59*, 984–1001; *Angew. Chem.* **2020**, *132*, 996–1013.
[25] S. Yannacone, V. Oliveira, N. Verma, E. Kraka, *Inorganics* **2019**, *7*, 47.
[26] M. Ochiai, T. Sueda, K. Miyamoto, P. Kiprof, V. V. Zhdankin, *Angew. Chem. Int. Ed.* **2006**, *45*, 8203–8206; *Angew. Chem.* **2006**, *118*, 8383–8386.
[27] a) P. K. Sajith, C. H. Suresh, *Inorg. Chem.* **2012**, *51*, 967–977; b) P. K. Sajith, C. H. Suresh, *Inorg. Chem.* **2013**, *52*, 6046–6054.
[28] M. Li, H. Zheng, X.-s. Xue, J.-p. Cheng, *Tetrahedron Lett.* **2018**, *59*, 1278–1285.
[29] H. Jiang, T.-Y. Sun, Y. Chen, X. Zhang, Y.-D. Wu, Y. Xie, H. F. Schaefer, *Chem. Commun.* **2019**, *55*, 5667–5670.
[30] S. Yannacone, K. D. Sayala, M. Freindorf, N. V. Tsarevsky, E. Kraka, *Phys. Chem.* **2021**, *1*, 45–68.
[31] E. Kraka, W. Zou, Y. Tao, *WIREs Comput. Mol. Sci.* **2020**, *10*, e1480.
[32] T.-Y. Sun, K. Chen, Q. Lin, T. You, P. Yin, *Phys. Chem. Chem. Phys.* **2021**, *23*, 6758–6762.
[33] A. Dasgupta, C. Thiehoff, P. D. Newman, T. Wirth, R. L. Melen, *Org. Biomol. Chem.* **2021**, *19*, 4852–4865.
[34] S. Koichi, B. Leuthold, H. P. Lüthi, *Phys. Chem. Chem. Phys.* **2017**, *19*, 32179–32183.
[35] K. Eskandari, H. Zariny, *Chem. Phys. Lett.* **2010**, *492*, 9–13.
[36] R. F. W. Bader, M. T. Carroll, J. R. Cheeseman, C. Chang, *J. Am. Chem. Soc.* **1987**, *109*, 7968–7979.
[37] a) Z. Konkoli, D. Cremer, *Int. J. Quantum Chem.* **1998**, *67*, 1–9; b) Z. Konkoli, J. A. Larsson, D. Cremer, *Int. J. Quantum Chem.* **1998**, *67*, 11–27; c) Z. Konkoli, D. Cremer, *Int. J. Quantum Chem.* **1998**, *67*, 29–40; d) Z. Konkoli, J. A. Larsson, D. Cremer, *Int. J. Quantum Chem.* **1998**, *67*, 41–55; e) D. Cremer, J. A. Larsson, E. Kraka, in *Theoretical and Computational Chemistry, Vol. 5* (Ed.: C. Párkányi), Elsevier, Amsterdam, **1998**, pp. 259–327.
[38] a) E. B. Wilson, J. C. Decius, P. C. Cross, Molecular vibrations : the theory of infrared and Raman vibrational spectra, McGraw-Hill, New York, **1955**; b) S. Califano, Vibrational States, Wiley, **1976**; c) G. Herzberg, Molecular spectra and molecular structure. II, Infrared and raman spectra of polyatomic molecules, Van Nostrand, New York, **1945**.
[39] W. Zou, D. Cremer, *Chem. Eur. J.* **2016**, *22*, 4087–4099.
[40] a) M. Freindorf, E. Kraka, *J. Mol. Model.* **2020**, *26*, 281; b) S. Yannacone, M. Freindorf, Y. Tao, W. Zou, E. Kraka, *Crystals* **2020**, *10*, 556; c) Y. Tao, L. Zhang, W. Zou, E. Kraka, *Symmetry* **2020**, *12*, 1545; d) A. A. A. Delgado, D. Sethio, I. Munar, V. Aviyente, E. Kraka, *J. Chem. Phys.* **2020**, *153*, 224303; e) Y. Tao, W. Zou, D. Sethio, N. Verma, Y. Qiu, C. Tian, D. Cremer, E. Kraka, *J. Chem. Theory Comput.* **2019**, *15*, 1761–1776; f) A. A. A. Delgado, A. Humason, R. Kalescky, M. Freindorf, E. Kraka, *Molecules* **2021**, *26*, 950; g) N. Beiranvand, M. Freindorf, E. Kraka, *Molecules* **2021**, *26*, 2268.
[41] a) M. Kaupp, D. Danovich, S. Shaik, *Coord. Chem. Rev.* **2017**, *344*, 355–362; b) E. Kraka, D. Cremer, *Rev. Proc. Quím.* **2012**, *6*; c) D. Setiawan, E. Kraka, D. Cremer, *J. Phys. Chem. A* **2015**, *119*, 9541–9556; d) E. Kraka, D. Setiawan, D. Cremer, *J. Comput. Chem.* **2016**, *37*, 130–142.
[42] a) E. Kraka, J. A. Larsson, D. Cremer, in *Computational Spectroscopy* (Ed.: G. J.), Wiley, New York, **2010**, pp. 105–149; b) R. Kalescky, E. Kraka, D. Cremer, *Int. J. Quantum Chem.* **2014**, *114*, 1060–1072; c) R. Kalescky, W. Zou, E. Kraka, D. Cremer, *J. Phys. Chem. A* **2014**, *118*, 1948–1963.
[43] E. Kraka, D. Cremer, in *Theoretical Models of Chemical Bonding. The Concept of the Chemical Bond, Vol. 2* (Ed.: Z. B. Maksic), Springer Verlag, Heidelberg, **1990**, pp. 453–542.
[44] R. F. W. Bader, H. Essén, *J. Chem. Phys.* **1984**, *80*, 1943–1960.
[45] S. Shaik, D. Danovich, W. Wu, P. C. Hiberty, *Nat. Chem.* **2009**, *1*, 443–449.
[46] S. Shaik, D. Danovich, B. Braida, W. Wu, P. C. Hiberty, in *The Chemical Bond II: 100 Years Old and Getting Stronger* (Ed.: D. M. P. Mingos), Springer International Publishing, Cham, **2016**, pp. 169–211.
[47] a) H. Pinto de Magalhães, H. P. Lüthi, P. Bultinck, *Phys. Chem. Chem. Phys.* **2016**, *18*, 846–856; b) S. Koichi, H. P. Lüthi, *Chimia* **2019**, *73*, 990–996.
[48] T.-Y. Sun, X. Wang, H. Geng, Y. Xie, Y.-D. Wu, X. Zhang, H. F. Schaefer Iii, *Chem. Commun.* **2016**, *52*, 5371–5374.
[49] K. B. Wiberg, *Tetrahedron* **1968**, *24*, 1083–1096.
[50] a) A. V. Marenich, C. J. Cramer, D. G. Truhlar, *J. Phys. Chem. B* **2009**, *113*, 6378–6396; b) E. Engelage, N. Schulz, F. Heinen, S. M. Huber, D. G. Truhlar, C. J. Cramer, *Chem. Eur. J.* **2018**, *24*, 15983–15987.
[51] Y. Zhao, D. G. Truhlar, *Theor. Chem. Acc.* **2008**, *120*, 215–241.
[52] F. Weigend, R. Ahlrichs, *Phys. Chem. Chem. Phys.* **2005**, *7*, 3297–3305.
[53] D. Rappoport, F. Furche, *J. Chem. Phys.* **2010**, *133*, 134105.
[54] K. A. Peterson, D. Figgen, E. Goll, H. Stoll, M. Dolg, *J. Chem. Phys.* **2003**, *119*, 11113–11123.
[55] T.-Y. Sun, K. Chen, H. Zhou, T. You, P. Yin, X. Wang, *J. Comput. Chem.* **2021**, *42*, 470–474.
[56] F. Weinhold, C. R. Landis, E. D. Glendening, *Int. Rev. Phys. Chem.* **2016**, *35*, 399–440.
[57] A. D. Becke, K. E. Edgecombe, *J. Chem. Phys.* **1990**, *92*, 5397–5403.
[58] N. Mohan, C. H. Suresh, *J. Phys. Chem. A* **2014**, *118*, 1697–1705.
[59] a) R. F. W. Bader, Atoms in Molecules: A Quantum Theory (International Series of Monographs on Chemistry), Clarendon Press, **1994**; b) P. L. P., Atoms in Molecules: An Introduction, Prentice Hall, **2000**.
[60] M. J. Frisch, G. W. Trucks, H. B. Schlegel, G. E. Scuseria, M. A. Robb, J. R. Cheeseman, G. Scalmani, V. Barone, G. A. Petersson, H. Nakatsuji, X. Li, M. Caricato, A. V. Marenich, J. Bloino, B. G. Janesko, R. Gomperts, B. Mennucci, H. P. Hratchian, J. V. Ortiz, A. F. Izmaylov, J. L. Sonnenberg,

Williams, F. Ding, F. Lipparini, F. Egidi, J. Goings, B. Peng, A. Petrone, T. Henderson, D. Ranasinghe, V. G. Zakrzewski, J. Gao, N. Rega, G. Zheng, W. Liang, M. Hada, M. Ehara, K. Toyota, R. Fukuda, J. Hasegawa, M. Ishida, T. Nakajima, Y. Honda, O. Kitao, H. Nakai, T. Vreven, K. Throssell, J. A. Montgomery Jr., J. E. Peralta, F. Ogliaro, M. J. Bearpark, J. J. Heyd, E. N. Brothers, K. N. Kudin, V. N. Staroverov, T. A. Keith, R. Kobayashi, J. Normand, K. Raghavachari, A. P. Rendell, J. C. Burant, S. S. Iyengar, J. Tomasi, M. Cossi, J. M. Millam, M. Klene, C. Adamo, R. Cammi, J. W. Ochterski, R. L. Martin, K. Morokuma, O. Farkas, J. B. Foresman, D. J. Fox, Wallingford, CT, **2016**.

[61] E. D. Glendening, C. R. Landis, F. Weinhold, *J. Comput. Chem.* **2013**, *34*, 1429–1437.

[62] T. Lu, F. Chen, *J. Comput. Chem.* **2012**, *33*, 580–592.

[63] W. Humphrey, A. Dalke, K. Schulten, *J. Mol. Graphics* **1996**, *14*, 33–38.

[64] T. A. Keith, AIMALL, Version 19.10.12, **2019**.

[65] W. Zou, Y. Tao, M. Freindorf, M. Z. Makos, E. Kraka, Computational and Theoretical Chemistry Group (CATCO), Southern Methodist University: Dallas, TX, USA, **2020**.

Manuscript received: June 19, 2021
Revised manuscript received: August 9, 2021
Accepted manuscript online: August 18, 2021